Physiological Regulation of the Immunological Synapse by Agrin

Adil A. Khan,[1,2]* Christian Bose,[2] Lung S. Yam,[2] Mark J. Soloski,[3] Fabio Rupp[2]†

T cell activation is dependent on both a primary signal delivered through the T cell receptor and a secondary costimulatory signal mediated by coreceptors. Although controversial, costimulation is thought to act through the specific redistribution and clustering of membrane and intracellular kinase-rich lipid raft microdomains at the contact site between T cells and antigen-presenting cells. This site has been termed the immunological synapse. Endogenous mediators of raft clustering in lymphocytes have not been identified, although they are essential for T cell activation. We now demonstrate that agrin, an aggregating protein crucial for formation of the neuromuscular junction, is also expressed in lymphocytes and is important in reorganization of membrane lipid microdomains and setting the threshold for T cell signaling. Our data show that agrin induces the aggregation of signaling proteins and the creation of signaling domains in both immune and nervous systems through a common lipid raft pathway.

The aggregation of surface molecules is a fundamental mechanism by which both lymphocytes and neurons regulate transmembrane signaling. In the immune system, the ligand-induced clustering of membrane lipid microdomains is an essential event in the focal transduction of intercellular signals that regulate lymphocyte activation, growth, and differentiation (*1*). Similarly, aggregation of pre- and postsynaptic molecules in the nervous system is essential for synapse formation and ensures the zonal and rapid exchange of information between neurons (*2*). One neuronal aggregating factor, a ~400-kD proteoglycan termed agrin for its ability to induce the aggregation of acetylcholine receptors (AChRs) and other postsynaptic proteins on muscle fibers, has been purified. Its clustering activity has been shown to be crucial for the formation of the neuromuscular junction (*3*). Agrin is secreted from motor neurons and acts extracellularly to trigger the local aggregation of proteins at the developing neuromuscular junction. Alternative splicing at a specific position in the agrin mRNA (position Z) results in the insertion of additional amino acids in agrin (Z^+ isoforms) and produces neuron-specific agrin polypeptides with varying aggregating activity (*4*). Splicing at the Z position does not occur in peripheral tissues (agrin Z^- isoforms), and the function of these broadly expressed agrin isoforms is not known.

Although receptor aggregation and lipid microdomain reorganization are also fundamental for immune activation, endogenous proteins capable of inducing receptor aggregation in lymphocytes have not been identified (*1*). T cell activation is initiated by the interaction of T cell receptors (TCRs) with peptides that are displayed on the surface of antigen-presenting cells (APCs) (*5*). Costimulatory signals (*6*) induce the recruitment of TCRs to lipid rafts and the clustering of rafts into a formed functional module polarized toward the APC (*7*). Rafts, detergent-insoluble glycosphingolipid-enriched membrane microdomains, are preformed 70-nm lipid assemblies rich in kinases and adapter molecules (*8*). Rafts serve as platforms for signal transduction and, in clustering, form the TCR-APC contact junction, termed the immunological synapse (*9*). This TCR-APC adhesion complex allows the concentration and exclusion of specific membrane proteins and permits sustained second-messenger generation crucial for T cell activation and clonal expansion (*9*). We now demonstrate that agrin, previously identified as an aggregating factor in the developing nervous system, exists in primary immunocytes and that when purified from activated lymphocytes can induce lipid raft reorganization and can regulate the threshold for lymphocyte activation.

Agrin is differentially expressed in resting and activated primary immune cells. Northern blot analyses using a full-length agrin cDNA probe detected an 8.0-kb band in mRNA isolated from primary adult rat thymocytes and splenocytes (Fig. 1A). Western blot analyses of protein extracts from the same cells using an agrin-specific monoclonal antibody (mAb) m33 (*10*) revealed a broad agrin-immunoreactive band of approximate molecular mass of 250 to 400 kD, suggesting extensive glycosylation, as previously reported for agrin in the nervous system (*11*) (Fig. 1B). To examine whether immune activation alters agrin expression, we performed Western blot analysis of concanavilin A (Con A)–activated splenocytes. In contrast to resting lymphocytes, m33 agrin immunoreactivity in Con A–activated cells was reduced to low levels (Fig. 1C). Northern analysis of resting and Con A–activated splenocytes and thymocytes indicated no change in agrin mRNA levels (*12*). We screened protein extracts from resting and Con A–activated splenocytes with a series of agrin mAbs that recognized different epitopes within agrin (*10*). Agrin m247 (*10*) recognized a sharp agrin-immunoreactive band of ~240 kD (Fig. 1C) in activated splenocytes and, in contrast to m33, did not recognize agrin in resting cells. By immunocytochemistry, m247 displayed low reactivity with agrin in resting splenocytes. After Con A–induced immune activation, m247 immunofluorescence increased with agrin immunoreactivity localized to clustered and capped membrane regions and colocalized with the TCR/CD3 signaling complex (Fig. 1D).

To determine which immune cells express agrin, we examined agrin expression in resting and Con A–activated thymocytes and splenocytes by using flow cytometry. Low levels of agrin are detected by m247 in resting thymocytes and this expression is confined to the $CD4^+/CD8^+$ subpopulation. However, after Con A treatment, agrin m247 immunoreactivity increased in discrete thymic subpopulations: $CD4^+/CD8^+$, $CD4^+/CD8^-$ cells and a subpopulation of $CD8^+/CD4^-$ cells expressed agrin, whereas $CD4^-/CD8^-$ cells did not. A subpopulation of resting $CD4^+/CD8^-$ splenocytes expressed low levels of agrin, although, after Con A stimulation, agrin immunoreactivity increased in all $CD4^+/CD8^-$ and $CD8^+/CD4^-$ cells. Resting B cells expressed low levels of agrin, which are also increased after brief Con A stimulation (Fig. 1E).

To further examine the relation between changes in agrin immunoreactivity and T cell activation, we performed Western blot analysis on protein extracts from mixed-lymphocyte reactions (MLR) (*13*). Whereas agrin m33 immunoreactivity decreased in activated lymphocytes within the first 12 hours of stimulation, reaching a low baseline level at 24 hours, agrin m247 immunoreactivity progressed from undetectable to maximal levels during the same stimulation period (Fig. 2A).

[1]Outer Banks Neuroscience, Baltimore, MD 21218, USA. [2]Department of Neuroscience, Johns Hopkins University School of Medicine, Baltimore, MD 21205, USA. [3]Department of Medicine, Johns Hopkins University School of Medicine, Baltimore, MD 21205, USA.

*To whom correspondence should be addressed: outerbanksneuro@yahoo.com

†Present address: Hyseq Inc., Sunnyvale, CA 94085, USA.

As with Con A–induced immune activation, immunofluorescence with m247 showed low agrin immunoreactivity in unstimulated cells but an increase in MLR-stimulated cells in clustered membrane regions and discrete cell-cell contact sites (Fig. 2B).

Purified agrin induces lipid raft aggregation and modulates the threshold for immune activation. Agrin m247 immunoreactivity in activated lymphocytes is localized to clustered and capped membrane regions. Because agrin induces the aggregation of AChR on the surface of myotubes (*4*), we asked whether agrin expressed in activated lymphocytes induces the aggregation of surface receptors essential for T cell activation. Signals from costimulatory molecules such as CD28 (*6*) recruit TCR/CD3 complexes to lipid rafts and activate an actin-myosin–driven transport process that mobilizes rafts to cell-cell contact sites (*14*). We tested whether agrin application affected the surface distribution of rafts by using the raft marker fluorescein isothiocyanate (FITC)-labeled cholera toxin B (CTx-B) subunit, which binds the glycosphingolipid G_{M1} (*15*).

Using m33 and m247 mAb immuno-affinity columns, we purified agrin from resting and Con A–activated splenocytes (*16*) (Fig. 3, A and B) and incubated primary cultures of thymocytes and splenocytes with picomolar concentrations of the purified agrin. In untreated resting T lymphocytes and in T cells treated with agrin purified from resting cells ($agrin_{rest}$), G_{M1} was evenly distributed along the cell surface (Fig. 3C). By contrast, in T cells treated with agrin purified from activated cells ($agrin_{act}$), G_{M1} was redistributed into clusters and dense caps (Fig. 3D). To confirm that the $agrin_{act}$-induced G_{M1} aggregation was due to a direct effect of $agrin_{act}$ on T cells, we purified T cells from cultured splenocytes (Fig. 3D). $Agrin_{act}$ lipid raft clustering activity is strikingly potent, with picomolar concentrations of $agrin_{act}$ required to cluster FITC–CTx-B staining. These $agrin_{act}$-induced G_{M1} raft clusters also contained other signaling molecules such as CD28 (Fig. 3E), CD3, and major histocompatibility complex (MHC) class I, as well as coclustering with the Lck tyrosine kinase (Fig. 3F). Although $agrin_{act}$-induced raft mobilization coclusters with immune signaling molecules, as shown in Fig. 3E, lipid rafts cluster independently in some cells.

To examine the functional role of $agrin_{act}$ in lipid raft aggregation during lymphocyte activation, we measured its ability to modulate the proliferation thresholds of splenocytes from mice transgenic for a TCR that recognizes chicken ovalbumin (OVA) in the context of I-A^d DO11.10 (*17*). Proliferation was measured by culturing splenocytes from transgenic mice with varying doses of OVA peptide in the presence of picomolar concentrations of purified $agrin_{act}$. Incubation with $agrin_{act}$ markedly lowered the OVA threshold for lymphocyte activation and decreased the magnitude of the response to saturating amounts of OVA (Fig. 4A). Incubation of splenocytes with $agrin_{act}$ in the absence of OVA did not induce proliferation.

We also examined the effects of agrin ligation on immune responses by measuring the proliferation thresholds of rat T lymphocytes cultured in the presence of incremental concentrations of the mAb against CD3 and a saturating concentration of the mAb against agrin. The threshold for proliferative responses elicited with the mAb against CD3 is markedly lowered, and the supra-threshold response is increased by the presence of the mAb against

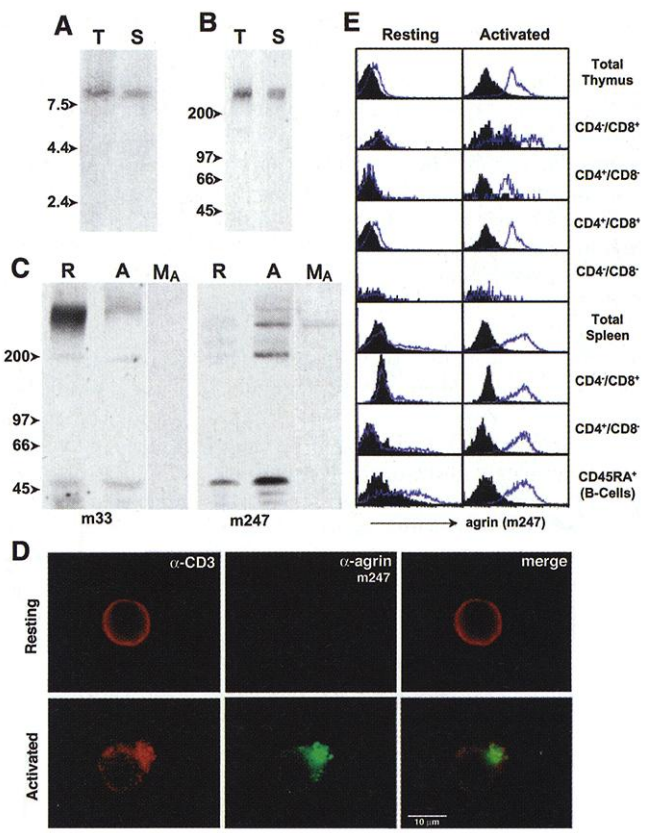

Fig. 1. Agrin is expressed in lymphocytes and, after immune activation, cocaps with the TCR/CD3 complex. (**A**) Detection of agrin by Northern blot analysis for mRNA in thymocytes (lane T) and splenocytes (lane S). An 18*S* RNA probe was used as a control for quantity of RNA. The full-length agrin probe detects a band at approximately 8.0 kb in both tissues. (**B**) Protein immunoblot detection of agrin in thymocytes and splenocytes with mAb m33. Molecular mass is shown at the left (in kilodaltons). (**C**) Western blot analysis of protein extracts from resting (lane R) and Con A–activated (lane A) splenocytes with agrin mAb m33 and m247. Lane M_A refers to cell culture medium analyzed from Con A–activated splenocytes. Agrin is not detected in cell culture medium from resting cells (*12*). Splenocytes, cultured in RPMI 1640 with FBS (10%), were incubated with Con A (10 μg/ml) for 3 hours. Similar results were obtained with resting and Con A–activated thymocytes. Con A treatment of immune cells induces surface receptor clustering and endocytosis. Agrin mAb 247 detects protein bands of 240-, 200-, and 45-kD in Con A–treated splenocytes (lane A). The 240-kD mAb 247 immunoreactive protein band is reflective of the core agrin protein size, and the 200- and 45-kD bands are proteolytic fragments of the 240-kD agrin core protein. Similar-sized agrin proteolytic fragments are seen in purified agrin preparations from the *Torpedo* (ray) electric organ (*4*). (**D**) Localization and topographical distribution of TCR/CD3 complex surface antigens (red/left panels) and agrin (green/middle panels) as shown by immunocytochemistry in resting (upper row) and Con A–treated splenocytes (lower row). Splenocyte cell suspensions in Hanks' basic salt solution, 1 mM Hepes, and FBS (2%) were stained with the m247 mAb against agrin and mAb against CD3 before and after a 3-hour exposure to Con A (10 μg/ml) and were analyzed by confocal microscopy. Resting splenocytes express low levels of agrin immunoreactivity (green/upper middle panel) as detected by the m247 mAb. Con A–activated splenocytes express agrin (green/lower middle panel) in compartmentalized membrane regions colocalized with the TCR/CD3 complex (merge/lower right panel). Areas of colocalization are indicated in yellow by the blending of red TCR/CD3 and green agrin m247. Similar results were obtained using agrin m247 mAb in combination with mAbs against CD4 or CD8 (*12*). (**E**) Resting splenocytes (left panels) or splenocytes activated with Con A for 3 hours (right panels) were stained with phycoerythrin (PE)-coupled mAb against CD4 (PharMingen), biotin-linked CD8 mAb for detection of T cell subsets, PE-coupled mAb against CD45RA (B cell specific, PharMingen), agrin m247 mAb (Stressgen) or control mAb followed by streptavidin PercP (Becton Dickinson) and FITC-labeled goat antibody against rat IgG. Triple- or double-stained cells were analyzed by using a FACScan cell analyzer (Becton Dickinson). Viable cells were gated using forward and side scatter. Displayed are the levels of background FITC-IgG staining (black) and specific agrin m247 mAb (purple) staining on total cell populations or on gated subsets. The experiments in Fig. 1 were repeated three times with similar results.

agrin (Fig. 4B). The mAb against agrin does not induce lymphocyte proliferation when added alone. To examine the enhanced proliferation after CD3 and agrin coligation in more detail, we cultured rat splenocytes with increasing concentrations of the mAb against CD3, and saturating concentration of the mAbs against both agrin and CD28 (*18*). Independent agrin ligation and CD28 engagement both reduced the threshold for CD3-mediated proliferation and were similar in potency. The stimulatory effects of agrin ligation and CD28 coreceptor engagement were not significantly additive when combined.

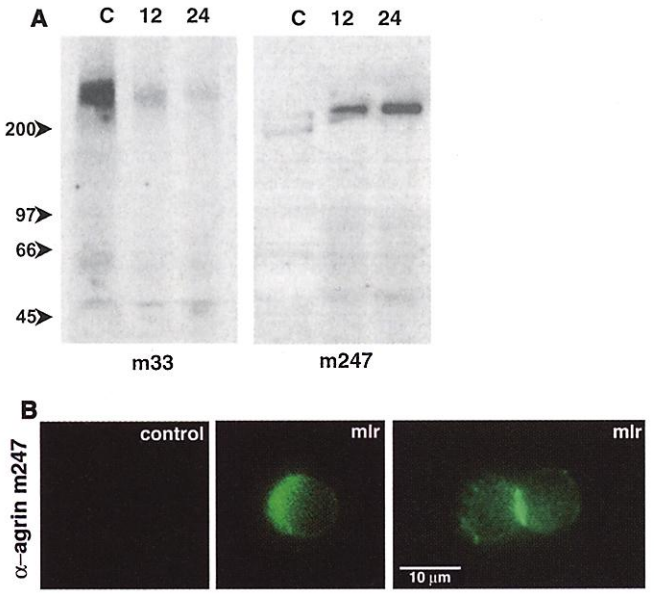

Fig. 2. Mixed-lymphocyte stimulation induces changes in agrin epitope expression similar to Con A activation. (**A**) Protein immunoblot detection of agrin with mAb m33 and m247 (left and right panels, respectively). Lanes C, 12, and 24 refer to 0, 12, and 24 hours after the onset of the mixed lymphocyte culture. Molecular mass is shown at the left (in kilodaltons). (**B**) Topographical distribution of agrin as shown by m247 mAb immunocytochemistry in resting and MLR-activated splenocytes. Resting splenocytes express low levels of agrin immunoreactivity as detected by the mAb m247 (left panel). Agrin immunofluorescence in MLR-activated lymphocytes is localized to compartmentalized cell membrane regions and cell-cell contact sites (middle, right panels). MLR splenocyte cell suspensions in Hanks' basic salt solution, 1 mM Hepes, and FBS (2%) were stained with the agrin mAb m247 before and after a 12-hour exposure to stimulator cells. These experiments were repeated three times with similar results.

The changes in agrin immunoreactivity during Con A– and MLR-induced immune stimulation, as detected by Western blot analysis using the m247 and m33 mAbs, occur over the course of several hours. Although the sampling intervals used for Western analysis reflect times for these nonspecific forms of immune stimulation to proceed to completion, we see changes in agrin m247 immunofluorescence in individual Con A–responsive lymphocytes within minutes of Con A treatment (*19*). To examine the kinetics of agrin activation more closely and to clarify its part in formation of the immunological synapse, we monitored the agrin m247 mAb and CTx-B immunofluorescence in cultured DO11.10 splenocytes after specific antigenic challenge with OVA. Immunocytochemistry with m247 mAb revealed low agrin immunoreactivity and uniform G_{M1} distribution in unstimulated splenocytes (Fig. 4C). However, several minutes after OVA administration an increase in m247 agrin immunoreactivity occurred, which was distributed along the cell

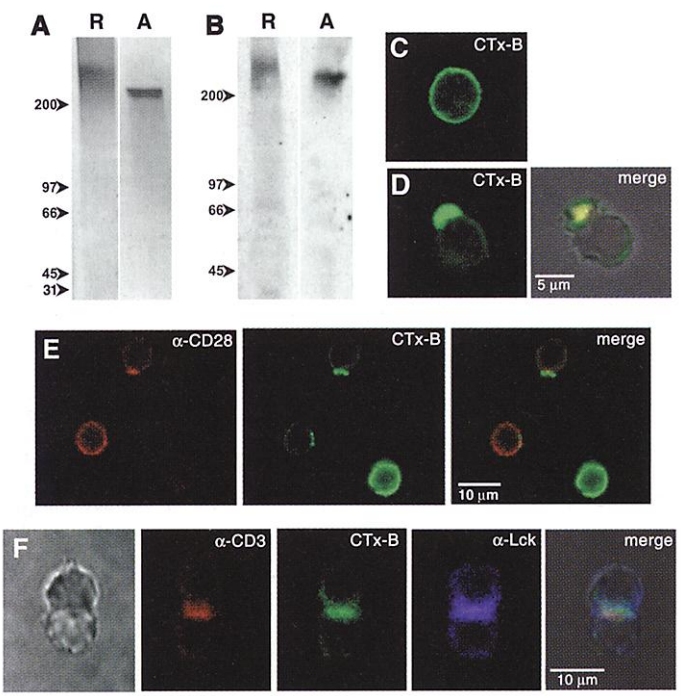

Fig. 3. Purified $agrin_{act}$ induces lipid raft redistribution, which is coclustered with T cell signaling molecules. (**A**) SDS-PAGE analysis of agrin purified from resting and Con A–activated splenocytes. A 4 to 16% polyacrylamide gel was silver stained. Lane R, ~10 ng purified $agrin_{rest}$; lane A, ~10 ng purified $agrin_{act}$. (**B**) Western blot analyses of agrin purified from resting (lane R) and Con A–activated (lane A) lymphocytes. Molecular mass is shown at the left (in kilodaltons). (**C**) Splenocytes treated with $agrin_{rest}$ and stained with FITC–CTx-B were analyzed by confocal microscopy. G_{M1} is uniformly distributed in cells treated with $agrin_{rest}$. Untreated resting splenocytes show the same uniform G_{M1} staining (*12*). (**D**) $Agrin_{act}$ induces lipid raft redistribution. FITC–CTx-B raft surface staining 15 min after treatment with $agrin_{act}$ is localized to compartmentalized membrane regions (left panel). $Agrin_{act}$ induces lipid raft clustering in purified T cells, indicating a direct activity of $agrin_{act}$ on T cells. Yellow indicates colocalization of CD3 complex surface antigens (red) and agrin (green) as shown by immunofluorescence in T cells treated with $agrin_{act}$ (right panel). (**E**) Colocalization and topographical distribution of CD28 surface antigens (red/left panel) and rafts (green/middle panel) as shown by immunofluorescence in splenocytes treated with $agrin_{act}$. Shown are the characteristic responses of cells in the same culture to $agrin_{act}$. In the top cell in panel (E), $agrin_{act}$ induces mobilization and cocapping of CD28 and raft staining (merge/right panel). In the left cell, raft staining has mobilized independently of CD28; in the cell at the lower right, lipid rafts are not mobilized (merge/right panel). Similar results after treatment with $agrin_{act}$ were obtained by using mAb against CD3 in combination with FITC–CTx-B (*12*). $Agrin_{act}$ treatment of resting splenocytes induces raft clustering and capping in 22 ± 5% (n = 4) of treated cells. This is compared with 6 ± 3% (n = 4) in cells treated with agrin purified from resting lymphocytes. Typically, Con A and antibody cross-linking treatments induce capping of surface receptors in 25 to 30% of cultured cells with 75% of cells unresponsive. This percentage is related to the cell-cycle phase of the treated cells (*18*). Experiments with synchronous cultures have indicated that capping is maximal in the G_2 phase and minimal in the G_1 and S phases of the cell cycle. The percentage of cultured cells responsive to agrin is in keeping with data indicating that rearrangement of membrane receptors can only occur at certain phases of the cell cycle. (**F**) Colocalization and topographical distribution of CD3 surface antigens (red/α-CD3), rafts (green/CTx-B), and Lck tyrosine kinase (blue/α-Lck) at an $agrin_{act}$-induced cell-cell contact site as shown by merged (right panel) immunofluorescence in splenocytes treated with $agrin_{act}$. Colocalization is indicated in white by the blending of red CD3, green raft, and blue Lck. Splenocyte cell suspensions in Hanks' basic salt solution, 1 mM Hepes, and FBS (2%) were stained with combinations of FITC–CTx-B, and mAbs against CD28, CD3, and Lck 15 min after exposure to $agrin_{act}$. The experiments in Fig. 3 were repeated three times with similar results.

surface of cultured splenocytes and colocalized with the raft marker FITC–CTx-B (Fig. 4C). Within 15 min after OVA addition, agrin m247 immunoreactivity clustered with membrane regions and discrete cell-cell contact sites, where it was colocalized with FITC–CTx-B (Fig. 4, D and E). Lipid rafts mobilize independently of agrin in some cells after OVA antigenic challenge (Fig. 4D). Although our results suggested that agrin in activated lymphocytes localized in lipid rafts, we also biochemically tested the relation between agrin and low-density, detergent-insoluble membranes in preparations from resting and activated splenocytes (Fig. 4F). Detergent extraction and Western blotting with the agrin m33 mAb show that virtually all the agrin in resting lymphocytes is soluble in 1% Triton X-100. In contrast, agrin m247 detects a sharp band at ~220 kD in 1% Triton extracts from Con A–activated splenocytes and also in detergent-insoluble fractions from activated cells, confirming the association of agrin with lipid rafts in activated lymphocytes.

Neuronal agrin induces lipid raft aggregation, which is colocalized with AChR clusters. In neurons, splicing at position Z in the agrin mRNA results in agrin polypeptides with aggregating activity (*4*). Reverse transcriptase–polymerase chain reaction (RT-PCR) analysis of RNA isolated from resting and activated lymphocytes detects exclusively agrin Z^- isoforms, confirming that alternative splicing at the Z position does not occur in the immune system (Fig. 5A). One difference between the pattern of agrin immunoreactivity in resting and activated lymphocytes was the apparent change in agrin molecular mass, detected by the agrin m33 and m247 mAbs; m33 detects a smeared pattern characteristic of heavily glycosylated proteins in resting lymphocytes, whereas m247 recognizes a sharp band, whose size reflected the core protein in activated lymphocytes (Figs. 1C, 2A, and 3, A and B). Our data suggest that the change in agrin immunoreactivity, as detected by agrin mAbs m33 and m247 in resting and activated lymphocytes, reflects the enzymatic deglycosylation of the resting agrin proteoglycan and not new protein synthesis of a deglycosylated agrin. Taken together, these results suggest that posttranslational modifications, and not alternative splicing, affect the aggregating activity of agrin expressed in lymphocytes. The change in pattern of agrin immunoreactivity detected by these two mAbs is consistent with prior work demonstrating extensive protein deglycosylation during lymphocyte activation (*20*).

Although splicing at the Z position in neurons affects the aggregating activity of agrin, the predominantly expressed neuronal agrin isoforms are not alternatively spliced (Z^-), are heavily glycosylated, and are inactive when added to the medium in AChR aggregation assays (*4*). To determine whether the protein modifications that occur during immune activation would confer AChR clustering activity to Z^- agrin isoforms, we treated myotube cultures with purified $agrin_{act}$ in myotube AChR aggregation assays. $Agrin_{act}$, but not $agrin_{rest}$, in-

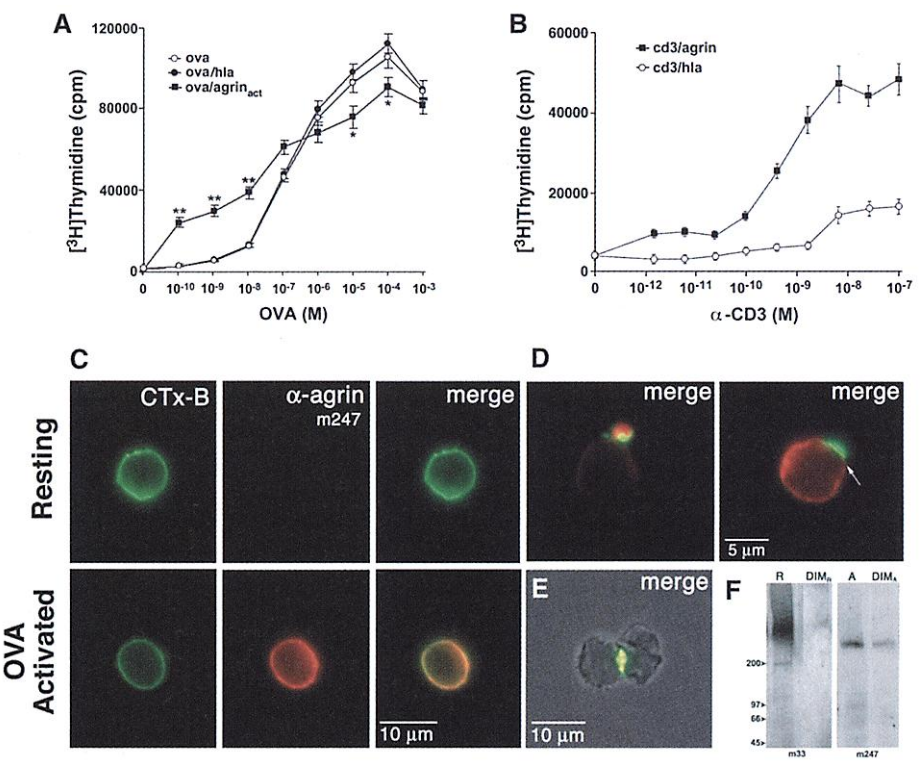

Fig. 4. (**A**) Antigenic reactivity of peripheral transgenic T cells to OVA peptide is enhanced by $agrin_{act}$. Splenocytes from H-2^d haplotype mice expressing the D011.10 αβ TCR were isolated and cultured at 2×10^6 cells per milliliter with the indicated concentration of OVA peptide. Proliferative responses of resting D011.10 splenocytes to OVA peptide (323 to 339) as a function of OVA concentration (●), and in the presence of picomolar concentrations of purified $agrin_{act}$ (■), or nonspecific antibody against human leukocyte antigen (HLA) (○). As a measure of lymphocyte proliferation, triplicate 200-μl cultures were pulsed with 1 μCi of [^{3}H]thymidine on the second day of a 3-day culture. Data represent the mean ± SEM of [^{3}H]thymidine uptake. Asterisks denote significant differences between control D011.10 OVA-treated splenocytes (●) and splenocytes cultured with OVA and purified $agrin_{act}$ (■) (**$P < 0.001$, *$P < 0.05$ t test). (**B**) Enhancement of DNA synthesis in rat splenocytes by the ligation of agrin. Proliferative responses of resting splenocytes to immobilized CD3 mAb as a function of CD3 mAb concentration in the presence of saturating amounts of agrin mAbs m33 and m247 (■) or nonspecific mAb against HLA (○). As a measure of lymphocyte proliferation, [^{3}H]thymidine uptake during the last 12 hours of a 4-day incubation was determined. Each point is the average of triplicate cultures, mean ± SEM. Round-bottom 96-well plates were coated with fourfold serial dilutions of mAb against rat CD3. Rat splenocytes (10^5) in Iscove's medium supplemented with 1 mM 2-mercaptoethanol, 10 mM Hepes, 2 mM glutamine, and antibiotics were cultured for 3 days in the presence of a saturating concentration (5 μg/well) of either both agrin m33 and m247 mAbs or nonspecific mAb against HLA. Cells were pulsed 12 hours with [^{3}H]thymidine (1 μCi/well) and harvested over glass fiber filters. (**C**) Antigenic challenge with OVA peptide induces agrin m247 mAb immunoreactivity. D011.10 splenocytes (10^6) were stained with FITC–CTx-B (green/left panel) and agrin m247 mAb (red/middle panel) before (upper row) and 5 min after administration of 1 μM OVA (lower row). Resting D011.10 splenocytes express low levels of agrin immunoreactivity (red/upper middle panel) as detected by the m247 mAb. OVA treatment of D011.10 splenocytes induces agrin immunoreactivity (red/lower middle panel), which is colocalized with FITC–CTx-B G_{M1} staining (merge/lower right panel). (**D**) Fifteen minutes after OVA addition, agrin m247 immunoreactivity is in clustered membrane regions, where it is colocalized with FITC–CTx-B (left panel). Lipid rafts mobilize independently of agrin in some cells after OVA antigenic challenge (right panel). Arrow indicates yellow area of lipid raft and agrin colocalization beneath green lipid raft cap. (**E**) In OVA-treated cells, agrin and the TCR/CD3 complex are coclustered at the interface between D011.10 T cells and APCs. Areas of colocalization are indicated in yellow by the blending of TCR/CD3 complex (red) and agrin m247 (green). (**F**) Agrin in activated lymphocytes localizes to low-density, detergent-insoluble membranes. Western blot analysis of 1% detergent extracts and low-density, detergent-insoluble membranes (*26*) from resting (lanes R and DIM_R) and Con A–activated (lanes A and DIM_A) splenocytes with agrin mAbs m33 and m247. Splenocytes, cultured in RPMI 1640 with FBS (10%), were incubated with Con A (10 μg/ml) for 1 hour. These experiments were repeated three times with similar results.

duced AChR clustering on myotubes, as detected by rhodamine-α-bungarotoxin binding. $Agrin_{act}$ treatment of myotubes also induced lipid raft mobilization. The AChR clusters on myotubes induced by $agrin_{act}$, as well as surface receptors aggregated in immune cells, were coclustered with the lipid raft marker FITC–CTx-B (Fig. 5, B and C). In neurons, agrin Z^+ isoforms induce AChR clustering. To determine whether neuron-specific agrin Z^+ isoforms would also induce raft microdomain clustering in conjunction with AChR aggregation, we treated myotube cultures with agrin Z^+ isoforms. As with $agrin_{act}$ (Z^-), neuronal agrin Z^+ polypeptides also induce raft mobilization on myotubes, which is colocalized with AChRs (Fig. 5D), suggesting a common raft-mediated aggregating mechanism.

In summary, we have established a novel role for agrin in immune synapses as an inducer of lipid raft aggregation. We demonstrate that picomolar concentrations of agrin purified from activated lymphocytes potently induce lipid raft clustering and membrane compartmentalization. Our results suggest that agrin activation, caused by engagement of immune signaling pathways, induces lipid raft redistribution and aids in the formation of the immunological synapse. This is supported by data indicating that $agrin_{act}$ is detected within minutes of antigenic challenge; purified picomolar concentrations of $agrin_{act}$ induce lipid raft reorganization; $agrin_{act}$-induced raft clustering dramatically decreases the threshold for antigen-induced lymphocyte proliferation.

The role of costimulatory molecules and raft clustering in lymphocyte activation is particularly relevant at suboptimal antigen concentrations or when the antigen receptor avidity is low. Costimulation, by initiating active directional transport of lipid raft domains to the area of cell-cell contact (*14*), may facilitate TCR-APC interaction by recruiting kinases and adhesion molecules into the cell-cell contact zone (*21*). This aids in bringing the membrane bilayers of the interacting cells together and may help overcome the weak avidity of the TCR for the small number of MHC-peptide complexes on APCs. $Agrin_{act}$-induced raft clustering and enhanced proliferation at suboptimal OVA concentrations in TCR transgenic mice splenocytes are in accord with a modulatory role for agrin in regulating the threshold for immune activation. At supra-threshold concentrations of OVA antigen, $agrin_{act}$ represses splenocyte proliferation. This inhibition may reflect a dual role for agrin in the formation and maintenance of the immunological synapse. Initially, the lipid raft aggregating activity of agrin triggers raft accumulation at cell-cell contact sites and promotes the formation of the immunological synapse. The time course of $agrin_{act}$ appearance after antigenic challenge and the raft-aggregating activity of picomolar concentrations of purified $agrin_{act}$ are consistent with a role for agrin in the formation of the immunological synapse. Although motor neuron agrin acts in a paracrine fashion, our results suggest that $agrin_{act}$ could act in both an autocrine and paracrine fashion. Once formed, the adhesive interaction between a single T cell–APC pair has a time course of several hours (*22*), although more dynamic interactions have been reported (*23*). This long-lasting contact is necessary to ensure the sustained signaling that maintains gene transcription, cell-cycle progression, and full T cell activation. $Agrin_{act}$, localized to the cell-cell contact interface, may also play a role in stabilizing the T cell–APC interaction over the course of the sustained cell union and eventually terminate signaling by endocytosis, allowing activated T cells to move freely from one APC to another. This is consistent with studies in the nervous system, which demonstrate that, in addition to agrin's receptor-aggregating activity, agrin and neural cell adhesion molecules are interactive partners (*12*).

Although the endogenous mechanisms that generate lipid raft assembly are still unknown, it is probable that raft aggregation and formation of the immunological synapse is regulated by receptors for aggregating ligands such as agrin. $Agrin_{act}$ may also enhance raft clustering in a lectin-like capacity, binding to and cross-linking carbohydrate moieties particular to rafts. Regulation of receptor clustering through differential glycosylation and lectin-like activity has been reported in *N*-acetylglucosaminyltransferase V (Mgat5)-deficient mice (*24*). Mgat5-dependent glycosylation limits raft clustering in control resting cells by promoting galectin-glycoprotein binding. Decreased galectin binding in Mgat5-deficient mice correlated with increased TCR clustering, suggesting the presence of a clustering inhibitory galectin-glycoprotein lattice in normal resting cells. Our results suggest that agrin promotes raft clustering after deglycosylation of the proteoglycan agrin during immune activation. It is possible that glycosylated agrin in resting cells may also dampen receptor clustering, which would be relieved following agrin deglycosylation or in agrin deficiency.

At the neuromuscular junction, agrin regulates the coaggregation of AChRs and other surface molecules such as α-sodium and Shaker-type K^+ channels (*3*, *25*). Our data show that neuronal Z^+ agrin also induces raft aggregation on myotubes, as well as clustering AChRs. Our results suggest that agrin-induced mobilization of lipid rafts reflects a conserved mechanism of receptor aggregation between immune and neural systems. Although the cargo of pro-

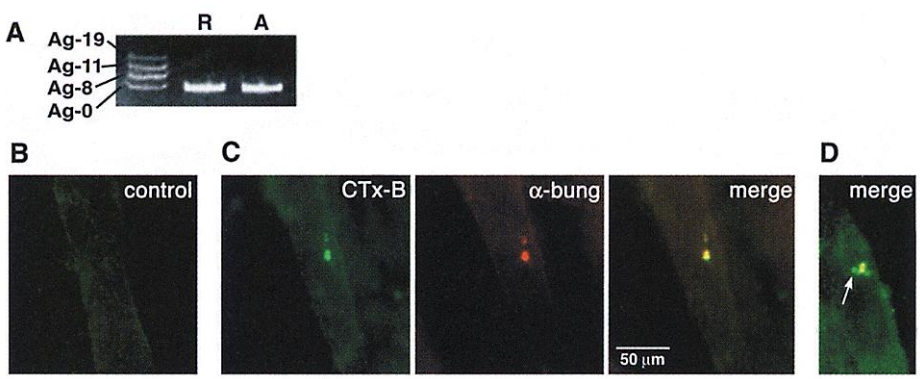

Fig. 5. (**A**) Immune activation does not alter agrin isoform expression. RT-PCR analyses of RNA samples isolated from resting splenocytes (lane R) and splenocytes treated with Con A for 3 hours (lane A). PCR products are separated on a 10% polyacrylamide gel (TAE) and visualized by ethidium bromide staining. Left lane, PCR products from cloned agrin isoforms (Ag-0, Ag-8, Ag-11, and Ag-19) differing at the Z position. The numbers (0, 8, 11, and 19) refer to the amino acid residue variants resulting from alternative splicing at the Z position of the agrin mRNA. Ag-8 and Ag-19 are approximately 10^3 times as efficient in aggregating AChR as the Ag-11 and Ag-0 (*4*). Similar results were obtained using RNA samples isolated from thymocytes. (**B**) Lipid rafts and AChRs are diffusely dispersed on resting myotubes. Fluorescence microscopy of lipid raft distribution (green) and AChR (red) on resting cultured C2 myotubes. (**C**) $Agrin_{act}$ induces raft mobilization and AChR clusters, which are colocalized on cultured myotobes. Fluorescence microscopy of raft mobilization (green/left panel) and AChR clustering (red/middle panel) on cultured C2 myotubes after a 3-hour exposure to purified lymphocyte $agrin_{act}$. Colocalization of lipid rafts and AChR clusters is shown in merged right panel. (**D**) Neuronal agrin Z^+isoforms also induce raft mobilization and AChR clusters, which are colocalized on cultured myotubes. Merged fluorescence microscopy of lipid raft (green) and AChR (red) coclusters on C2 myotubes after a 3-hour exposure to Z^+ agrin (*4*, *8*). Arrow indicates green lipid raft cluster not colocalized with AChR, suggesting protein heterogeneity between raft clusters. In panels (B), (C) and (D), AChR clusters were visualized using rhodamine-α-bungarotoxin (red); raft clusters were visualized with FITC–CTx-B (green). The experiments in Fig. 5 were repeated three times with similar results.

teins in the rafts is different in the two situations, the use of rafts as delivery vehicles and the regulation of their clustering by agrin may represent a general mechanism by which functional concentration of signaling molecules is achieved.

References and Notes

1. S. J. Singer, *Science* **255**, 1671 (1992).
2. Z. W. Hall, J. R. Sanes, *Cell* **72**, 99 (1993).
3. J. R. Sanes, J. W. Lichtman, *Annu. Rev. Neurosci.* **22**, 389 (1999).
4. M. Ferns *et al.*, *Neuron* **8**, 1079 (1992).
5. B. Malissen, A. M. Schmitt-Verhulst, *Curr. Opin. Immunol.* **5**, 324 (1993).
6. D. J. Lenschow, T. L. Walunas, J. A. Bluestone, *Annu. Rev. Immunol.* **14**, 233 (1996).
7. C. Montixi *et al.*, *EMBO J.* **17**, 5334 (1998).
8. R. G. Parton, K. Simons, *Science* **269**, 1398 (1995).
9. S. K. Bromley *et al.*, *Annu. Rev. Immunol.* **19**, 375 (2001).
10. Monoclonal antibodies were generated by W. Hoch *et al.* [*EMBO J.* **13**, 2814 (1994)] against the COOH-terminal half of agrin by immunizing several mice with an agrin fragment purified from transfected CHO cells. The binding site of the antibodies on agrin was determined by immunolabeling COS cells transfected with different agrin deletion constructs. Agrin mAb m33 has been mapped near the second laminin domain homology region and detects all agrin isoforms. Agrin m247 binds to an epitope close to splicing site Z. Agrin mAbs are commercially available through StressGen Biotechnologies, Victoria, Canada.
11. G. Tsen, W. Halfter, S. Kroger, G. J. Cole, *J. Biol Chem* **270**, 3392 (1995).
12. A. A. Khan, F. Rupp, unpublished data.
13. D. E. Mosier, *J. Immunol.* **112**, 305 (1974). The MLR was performed by using mitomycin C–treated (25 mg/ml) spleen cells from Brown Norway rats (stimulators) and splenocytes from Sprague-Dawley rats (responders).
14. C. Wülfing, M. M. Davis, *Science* **282**, 2266 (1998).
15. A. Schon, E. Freire, *Biochemistry* **28**, 5019 (1989).
16. Thymuses from 16 adult male (150 to 250 g) Sprague-Dawley rats were disassociated into single-cell suspensions in RPMI 10% fetal bovine serum (FBS). Half of the thymocyte cell suspension was untreated, and half was treated with Con A (10 μg/ml). Resting control thymocytes and thymocytes treated with Con A (10 μg/ml, 1 hour, 37°C) were washed in serum-free medium and pelleted. Cell pellets were frozen and thawed into buffer containing 50 mM Tris (pH 7.4) and protease inhibitors benzamidine (360 μg/ml), leupeptin (4 μg/ml), aprotinin (4 μg/ml), and pepstatin (4 μg/ml). Cell extracts were ground in a Dounce homogenizer and centrifuged at 35,000*g* for 45 min, and the subsequent supernatants were applied to agrin m247 and m33 immunoaffinity columns. Monoclonal agrin antibodies m33 and m247 in ascites fluid (Stressgen) were purified using Affi-Gel protein A agarose (Bio-Rad) and immobilized on Affi-Gel Hz hydrazide gel (Bio-Rad). Cell extracts were applied to the columns and washed with high-salt [phosphate-buffered saline (PBS, 0.5 M NaCl)] and low-salt (PBS, 0.15 M NaCl) buffers. Bound agrin was eluted with 0.2 M glycine-HCL, pH 2.5, and neutralized. Protein assays were performed according to directions for Pierce Coomassie blue. We used agrin's lipid raft aggregating activity to determine the multiple purification of agrin from starting thymocyte extracts to agrin immunoaffinity eluates; specific activity equivalent to agrin's lipid raft aggregating activity per amount of protein. We purified agrin 10,000-fold to homogeneity as detected by silver stain of protein resolved by SDS–polyacrylamide gel electrophoresis (SDS-PAGE). The concentration of agrin in assays was based on the molecular mass of agrin, the volume of the assay, and the amount of agrin purified from agrin immunoaffinity columns.
17. K. M. Murphy, A. B. Heimberger, D. Y. Loh, *Science* **250**, 1720 (1990).
18. Supplementary material, Web fig. 1, is available on *Science* Online at www.sciencemag.org/cgi/content/full/1056594/DC1
19. S. Lustig, D. H. Puznick, *J. Cell Physiol.* **115**, 87 (1983).
20. N. Razi, A. Varki, *Proc. Natl. Acad. Sci.* **95**, 7469 (1998).
21. A. Viola, S. Schroeder, Y. Sakakibara, A. Lanzavecchia, *Science* **283**, 680 (1999).
22. M. L. Dustin, A. C. Chan, *Cell* **103**, 283 (2000).
23. M. Gunzer *et al.*, *Immunity* **13**, 323 (2000).
24. M. Demetriou, M. Granovsky, S. Quaggin, J. W. Dennis, *Nature* **409**, 733 (2001).
25. G. Lück, W. Hoch, C. Hopf, D. Blottner, *Mol. Cell. Neurosci.* **16**, 269 (2000).
26. Splenocytes from eight adult male (150 to 250 g) Sprague-Dawley rats were isolated by Ficoll-hypaque and cultured in RPMI 10% FBS. Half of the splenocyte cell suspension was untreated, and half was treated with Con A (10 μg/ml). Resting control splenocytes and splenocytes treated with Con A (10 μg/ml, 1 hour, 37°C) were washed in serum-free medium and pelleted. Cell pellets were frozen and thawed into buffer containing 50 mM Tris (pH 7.4), and protease inhibitors benzamidine (360 μg/ml), leupeptin (4 μg/ml), aprotinin (4 μg/ml), and pepstatin (4 μg/ml). After centrifugation at 800*g* at 4°C for 10 min, the postnuclear supernatant was incubated with Triton X-100 at a final concentration of 1% for 30 min at 4°C. The lysate was adjusted to 1.3 M sucrose, placed at the bottom of a step sucrose gradient (0.2 to 0.9 M), and centrifuged (38,000 rpm, 15 hours).

27. We thank C. Hopf, R. Schnaar, and S. H. Snyder for critically reviewing the manuscript, R. Tracey, Registered Biological Photographer, for graphic art, and M. Khan for insightful discussions. This work was supported in part by grants from the E. A. and J. Klingenstein Fund (F.R.), the Council for Tobacco Research (F.R.), and from the NIAID (R01AI20922 to M.J.S.).

16 October 2000; accepted 25 April 2001
Published online 10 May 2001;
10.1126/science.1056594
Include this information when citing this paper.

REPORTS

Evidence for Dust Grain Growth in Young Circumstellar Disks

Henry B. Throop,[1]* John Bally,[2] Larry W. Esposito,[1] Mark J. McCaughrean[3]

Hundreds of circumstellar disks in the Orion nebula are being rapidly destroyed by the intense ultraviolet radiation produced by nearby bright stars. These young, million-year-old disks may not survive long enough to form planetary systems. Nevertheless, the first stage of planet formation—the growth of dust grains into larger particles—may have begun in these systems. Observational evidence for these large particles in Orion's disks is presented. A model of grain evolution in externally irradiated protoplanetary disks is developed and predicts rapid particle size evolution and sharp outer disk boundaries. We discuss implications for the formation rates of planetary systems.

The growth of dust grains orbiting young stars represents the first stage of planet formation (*1*). However, stars born in massive star-forming regions such as the Orion nebula are heated by intense ultraviolet (UV) radiation from nearby O and B stars, and the gas and dust in their disks can be lost in less than 10^5 years (*2*). Planet formation in such environments may therefore be inhibited if it requires substantially longer time than this (*3*). But, if growth to large particles can occur before removal of the gas and small particles, planets may nevertheless form from these disks. In this report, visual and near-infrared (IR) wavelength images obtained with the Hubble Space Telescope (HST) are used to show that particles in Orion's largest disk have grown to radii larger than 5 μm. Furthermore, the absence of millimeter-wavelength emission may provide evidence that grains have grown to sizes larger than a few millimeters. We develop a grain evolution model incorporating the effects of photoablation that demonstrates that the time scale for grain growth can be shorter than the photoevaporation time. It is thought that the majority of stars in the Galaxy form in photoevaporating regions such as the Orion nebula (*4*); if this is true, then giant planets and Kuiper belts of icy bodies around stars are probably rare unless they are formed very rapidly.

Solar system–sized circumstellar disks in the Orion nebula were first inferred from radio observations of dense ionized regions surrounding young low-mass stars (*5*). HST

[1]Laboratory for Atmospheric and Planetary Sciences, University of Colorado, Boulder, CO 80309–0392, USA. [2]CASA, University of Colorado, Boulder, CO 80309–0389, USA. [3]Astrophysikalisches Institut Potsdam, An der Sternwarte 16, D-14482 Potsdam, Germany.

*Present address: Southwest Research Institute, 1050 Walnut Street, Suite 426, Boulder, CO 80302, USA. E-mail: throop@boulder.swri.edu